

# A Radiative Flamelet Combustion Model For Turbulent, Premixed Methane-Air Flames

Cai Y. Ma

School of Chemical and Process  
Engineering  
University of Leeds, UK  
c.y.ma@leeds.ac.uk

Tariq Mahmud

School of Chemical and Process  
Engineering  
University of Leeds, UK  
t.mahmud@leeds.ac.uk

Michael Fairweather

School of Chemical and Process  
Engineering  
University of Leeds, UK  
m.fairweather@leeds.ac.uk

**Abstract**—The effect of radiation heat loss has been incorporated into a stretched laminar flamelet model of turbulent premixed flames using the enthalpy defect approach, and the method applied to the simulation of a number of stoichiometric methane-air jet flames. Comparison of predictions with available data on flames burning in the flamelet regime demonstrate that the model successfully captures the major features of these flames, in terms of flame position and velocity, temperature and major chemical species mass fraction fields, with satisfactory agreement with data for NO levels in one of the flames also being obtained. Overall, the model produces encouraging results for the flames examined, although further validation is required against measurements in idealised and practical burner configurations where the effects of thermal radiation heat loss are more evident.

**Keywords**—turbulent flow; premixed flames; jets; CFD; flamelet model; thermal radiation; nitric oxide

## I. INTRODUCTION

Mathematical models are now used increasingly in the design and performance prediction of burners employed, for example, in industrial boilers and furnaces. These models are used routinely to assist in burner design, and to ensure that high combustion efficiencies are achieved and that the level of pollutant emissions complies with legislation. For emissions of NO<sub>x</sub> in particular, predictive accuracy critically depends on the accuracy of temperature and oxygen concentration results derived from such models.

Many of the burners employed in industrial combustion equipment, including low NO<sub>x</sub> gas turbine combustors, use premixed fuel-air mixtures. A wide variety of combustion modelling approaches is available for predicting the turbulent reacting flows of interest (see, for example<sup>1</sup>). One such approach is the use of stretched laminar flamelet models<sup>2,3</sup> that account for the influence of high turbulence strain rates in quenching a flame. Bradley et al.<sup>4</sup> applied this concept to turbulent non-premixed combustion in the form of a mixedness-reactedness flamelet model which is based on the use of stretched laminar premixed, rather than diffusion, flamelets, with the parameters mixedness and reactedness quantifying, respectively, the degree of premixing before reaction

occurs and the completeness of combustion. This model has been applied successfully in computations of a wide range of turbulent, non-premixed flames (see, for example<sup>4,5</sup>), as well as being extended to cover turbulent premixed systems<sup>3</sup>.

It is well known that thermal radiation plays an important role in practical flames. In previous applications of flamelet models to turbulent flames, however, radiation heat loss has largely been unaccounted for (see, for example<sup>3,6</sup>) as the assumption of adiabatic combustion is generally invoked. The neglect of thermal radiation has led to the significant over prediction of temperatures in flames, particularly non-premixed, where radiation is important, and as a consequence the erroneous prediction of NO<sub>x</sub> levels that are highly temperature dependent. This restricts the range of applicability of flamelet models to flames with negligible radiation heat losses.

The present paper describes the development and application of a novel, non-adiabatic flamelet model that incorporates radiation heat loss effects into the calculation of turbulent premixed flames. The incorporation of such effects is particularly important in applications where the close proximity of solid surfaces, for example in boilers, causes significant radiation heat transfer from the flame and within the enclosure of the combustion device. The effect of radiation heat transfer is incorporated into the flamelet modelling methodology using the concept of enthalpy defect<sup>7</sup>. This parameter, defined as the difference between the actual enthalpy and the adiabatic enthalpy of a flame, is introduced as an additional flamelet variable. In the context of the premixed flamelet modelling approach<sup>3</sup>, the heat release rate in a laminar flame can then be expressed as a function of reactedness and enthalpy defect. A non-adiabatic flamelet data library has been generated using the CHEMKIN code<sup>8</sup> for one-dimensional laminar premixed flame calculations using a detailed chemical kinetic mechanism involving 49 species and 279 reaction steps. The CHEMKIN code has been modified by adding a source term to the energy conservation equation to account for radiation heat loss. Radiation heat transfer in turbulent flames is modelled by assuming the flames to be optically thin, with the wide-band model<sup>9</sup> used to determine the absorption coefficients of the radiating species. The complete methodology has been incorporated into the

stretched laminar flamelet model of Bradley et al.<sup>3</sup> for turbulent premixed combustion.

The performance of the non-adiabatic flamelet combustion model has been evaluated by computing the turbulent, stoichiometric premixed methane-air jet flames studied experimentally in<sup>10,11</sup>. Predictions of the combustion model, coupled to round jet calculations based on the  $k$ - $\varepsilon$  turbulence model, are compared with measurements.

## II. MODEL FORMULATION

An existing computer code, originally developed by Bradley and co-workers<sup>4</sup>, for the calculation of velocity and temperature fields in combustions flows using the stretched laminar flamelet approach, and later modified by Ma et al.<sup>5</sup> to include the species conservation equations, was employed in this study. The calculation procedure is based on the solution of the Favre-averaged conservation equations for mass, momentum, thermal energy and chemical species. Turbulence is handled using the  $k$ - $\varepsilon$  model, with standard values of the model constants<sup>12</sup>.

The temperature distribution is obtained by solving the thermal energy equation, modelled in terms of the sensible enthalpy. The source terms in this equation represent the turbulent mean volumetric heat release rate due to combustion and the volumetric heat loss due to thermal radiation. Radiative heat transfer was modelled by assuming the unconfined flames studied experimentally to be optically thin. Data for the absorption coefficients of the radiating species CH<sub>4</sub>, CO, CO<sub>2</sub> and H<sub>2</sub>O given by Tien<sup>9</sup>, and based on the wide-band model, were used in the present calculations.

The major chemical species concentration distributions were obtained from solutions of their transport equations. The mean reaction rate source term in these equations, and the turbulent mean volumetric heat release rate source term in the sensible enthalpy equation, were prescribed by the combustion model employed which is described below. NO concentrations were calculated using a post-processing approach<sup>13</sup> that involves the solution of the conservation equation for NO. The time-mean reaction rate of NO in the source term of this equation was obtained using a probability density function (PDF) approach, with the thermal-NO formation rate being determined using the Zeldovich mechanism<sup>14</sup> and the prompt-NO formation rate by a global rate expression from De Soete<sup>15</sup>.

The adiabatic flamelet combustion model<sup>3</sup>, applicable to turbulent premixed flames, was extended to take into account the effect of radiative heat transfer using the enthalpy defect concept<sup>7</sup>. The enthalpy defect is caused by the radiative heat loss,  $q_r$ , which is then imposed on the flamelets as a parameter. The turbulent mean heat release rate under non-adiabatic conditions is expressed as:

$$\bar{q}_t = P_b \int_0^1 \int_0^{q_r^{\max}} q_l(\theta, q_r) p(\theta, q_r) dq_r d\theta \quad (1)$$

where  $q_l(\theta, q_r)$  is the laminar volumetric heat release rate,  $\theta (= [T - T_u] / [T_m - T_u])$  the reactedness (a

reaction progress variable),  $T_u$  the unburnt gas temperature,  $T_m$  the maximum temperature of the premixture,  $p(\theta, q_r)$  is a joint probability density function of  $\theta$  and  $q_r$ , and  $P_b$  is the probability that the stretch rate can sustain a flamelet. By assuming statistical independence between  $\theta$  and  $q_r$ , and neglecting the effect of  $q_r$  fluctuations<sup>4,6</sup>, the joint PDF can be expressed as:

$$p(\theta, q_r) = p(\theta) \delta(q_r - \bar{q}_r), \quad (2)$$

where  $p(\theta)$  is represented by a beta-function and  $\delta(q_r - \bar{q}_r)$  is a delta-function. This joint PDF treatment is consistent with the assumptions made in the original flamelet model<sup>3</sup>. The turbulent mean heat release rate is then:

$$\bar{q}_t = P_b \int_0^1 q_l(\theta, \bar{q}_r) p(\theta) d\theta. \quad (3)$$

The beta-function PDF of  $p(\theta)$  was determined from the Favre mean values and variances of  $\theta$  which were obtained by solving their own modelled transport equations<sup>3</sup>. A similar approach was adopted to account for the effect of radiative heat transfer on the mean reaction rates.

For the methane-air flames<sup>10,11</sup> considered in this study, the laminar volumetric heat release rate and reaction rate data were generated from extensive calculations of one-dimensional premixed methane-air flames with a detailed chemical mechanism using the CHEMKIN code<sup>8</sup>. The GRI-Mech 2.11 reaction mechanism<sup>16</sup>, which involves 49 species and 279 reaction steps, was employed. For the generation of a non-adiabatic flamelet data library, the CHEMKIN code was modified by introducing a source term,  $q_r$ , into the energy conservation equation to account for radiative heat loss. The heat loss term  $q_r$  can be considered as an independent parameter that corresponds to the enthalpy defect. Fig. 1 shows calculated heat release rate profiles for a laminar, stoichiometric ( $\phi = 1$ ) premixed methane-air flame for different values of radiative heat loss. Similar profiles were generated for reaction rate data. The computed values of  $q_l(\theta, q_r)$  and the reaction rate parameter,  $w_{i,l}(\theta, q_r)$  were then curve fitted against  $\theta$  for each value of  $q_r$  in order to reduce computer storage requirements and significantly decrease model run times. The fits adopted were of the same form as those used by Bradley et al.<sup>4</sup> which provided a close fit to  $q_l(\theta, q_r)$  and  $w_{i,l}(\theta, q_r)$  values that had a close to Gaussian form. For chemical species, this meant that profiles of CH<sub>4</sub>, CO<sub>2</sub>, H<sub>2</sub>O and O<sub>2</sub> could be represented to a high degree of accuracy, whilst those of CO, H<sub>2</sub> and OH could not due to their non-Gaussian distribution. Given the current stage of development of the combustion model, the latter species were therefore excluded from the present study, although future work will address this shortcoming.

The Favre-averaged conservation equations, written in cylindrical co-ordinates for solution, were discretised by integrating over control volumes covering the computational domain. The convection terms were approximated by a third-order accurate,

non-diffusive, boundedness-preserving discretisation scheme<sup>17</sup>, while the diffusion terms were approximated using central differencing. The discretised equations were then solved by a variant<sup>17</sup> of the SIMPLE algorithm<sup>18</sup> that uses the pentadiagonal-matrix-algorithm.

### III. EXPERIMENTAL AND COMPUTATIONAL DETAILS

The first premixed stoichiometric methane-air jet flame<sup>10</sup> considered, referred to below as Case I, was produced by a 12 mm diameter burner with an exit flow Reynolds number of 21,000. Pilot flames which surrounded the main burner tube were used to stabilise the primary flame. A staggered, non-uniform, 77 (axial) × 68 (radial) computational mesh was used in calculating this flame following grid independence tests. Computations started 0.5 mm above the nozzle exit plane where normalised mean axial and fluctuating axial and radial velocities values were available from measurements. The mean radial velocity was set to zero at this location. The inlet values of the turbulence kinetic energy were calculated from measured fluctuating velocities with the assumption of the fluctuating azimuthal velocity being equal to the fluctuating radial velocity. The inlet turbulence energy dissipation rate was then determined from inlet turbulence kinetic energy values using an experimentally determined lateral integral length scale of 2.4 mm<sup>10</sup>. Similar calculations were also performed for a Re = 35,000 flame considered by the same authors, referred to below as Case II.

The second stoichiometric methane-air jet flame<sup>11</sup> considered, referred to as Case III, was produced by a burner of 8 mm diameter with Re = 8,000 at the nozzle exit. Computations were carried out on a staggered, two-dimensional, non-uniform mesh containing 107 (axial) × 127 (radial) nodes, with a higher mesh density in the region near the burner exit and close to the jet axis. Test calculations with different mesh sizes (between 59 × 75 and 140 × 180) again showed that the selected mesh was sufficiently fine to provide acceptable grid independent solutions. Inlet mean velocity data at the burner exit required for the calculations were obtained from measurements<sup>11</sup>, with the exit profile consisting of a high velocity central core and a surrounding low velocity region used to decrease the velocity gradient to the stagnant surroundings. The radial velocity was taken as zero, and the turbulence kinetic energy was determined by assuming 6% turbulence intensity, corresponding to a fully developed turbulent pipe flow. For this case, the inlet value of the turbulence kinetic energy dissipation rate was then evaluated from the turbulence kinetic energy using a length scale corresponding to 0.33 times the radius of the burner tube.

### IV. RESULTS AND DISCUSSION

Predictions and measurements of the mean axial velocity, mean temperature and fuel (i.e. CH<sub>4</sub>) concentration at four downstream locations (for axial distance x and burner diameter D) along the axis of the Case I flame are given in Fig. 2. Equivalent results

for the major species concentrations CO<sub>2</sub>, O<sub>2</sub> and H<sub>2</sub>O are shown in Fig. 3. Compared to a non-reacting flow, for which experimental data are available<sup>10</sup>, gas expansion within the flame results in higher axial velocities due to heat release. As a result of this expansion, the shear layer, located at the position of the maximum axial velocity gradient in the radial direction, is moved away from the centre-line, while the mean flame-front position moves towards the centre-line with increasing downstream distance because of the consumption of unburned mixture. All of these features were successfully reproduced by the present non-adiabatic flamelet model. The predictions of mean axial velocity are more diffuse than the measurements at the interface between the main flame jet and the co-flow of combustion products from the pilot flame used in the experimental configuration<sup>10</sup>. It is known, however, that such diffuse profiles occur even in constant density jet calculations that employ the standard *k-ε* turbulence model. This discrepancy is not, therefore, necessarily a result of the combustion model.

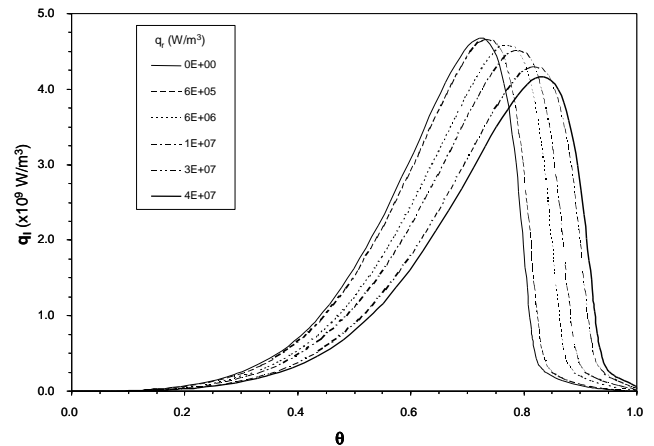


Fig. 1. Calculated heat release rate profiles for a laminar premixed methane-air flame ( $\phi = 1$ ) for different values of radiative heat loss ( $q_r$ ).

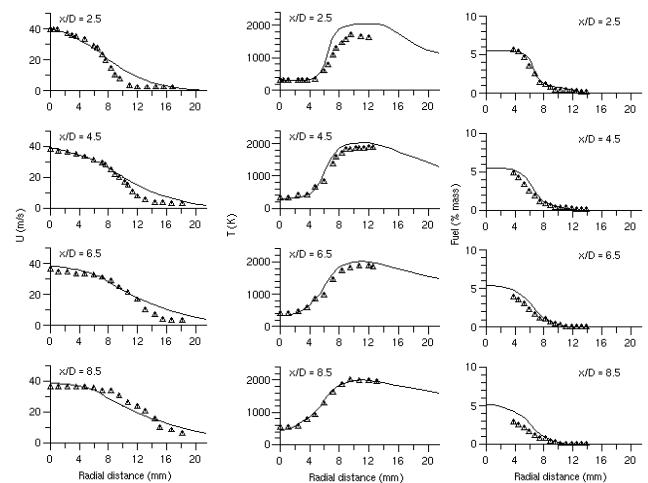


Fig. 2. Comparison of measured<sup>10</sup> and predicted mean axial velocities, temperatures and fuel concentrations at four downstream locations in the Case I flame (symbols - data, line - predictions).



The spreading rate of the flame is more accurately predicted by the results obtained for temperature, fuel and major species mass fractions. Predictions of mean temperatures are in close accord with data, although some slight over prediction does occur at the location closest to the burner. Likewise, predictions of  $\text{CH}_4$ ,  $\text{CO}_2$ ,  $\text{O}_2$  and  $\text{H}_2\text{O}$  are again in good agreement with data in terms of flame location and spreading rate, although a slight under estimation of peak  $\text{CO}_2$  and  $\text{H}_2\text{O}$  values is seen at all measurement stations, particularly towards the edge of the flame, with a corresponding over prediction of  $\text{O}_2$  levels also occurring. Additionally, at the first measurement location in particular, data for  $\text{CO}_2$  and  $\text{H}_2\text{O}$  are seen to be almost flat in the outer regions of the flow. This is most likely due to contributions from the burnt products of the pilot flame that were not modelled explicitly in the present work. This contribution is, however, generally small, and does not detract from the acceptable level of agreement obtained between predicted and observed results.

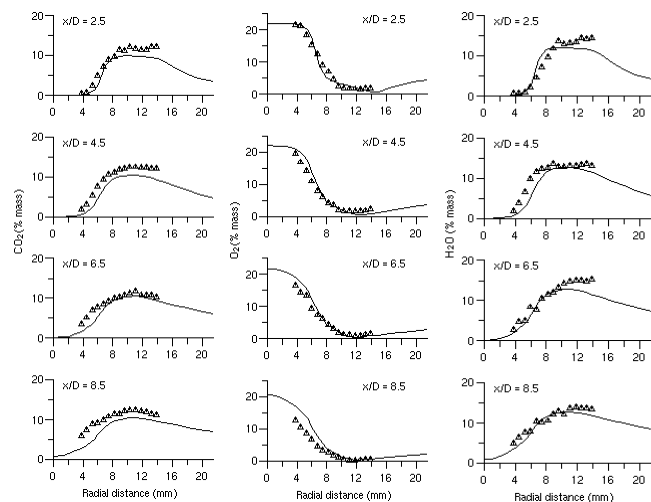


Fig. 3. Comparison of measured<sup>10</sup> and predicted  $\text{CO}_2$ ,  $\text{O}_2$  and  $\text{H}_2\text{O}$  levels at four downstream locations in the Case I flame (symbols - data, line - predictions).

Chen et al.<sup>10</sup> also presented two more data sets obtained using the same piloted burner, but with higher Reynolds numbers of 35,000 and 45,500. The non-adiabatic flamelet model was also applied to simulate these two flames, but the predicted results for these cases compared less favourably with experimental data. As an example, predictions and measurements for the  $\text{Re} = 35,000$ , Case II flame, are shown in Figs. 4 and 5. It can be seen that the trends of temperatures, axial velocities and major species concentrations of this flame have been duplicated well by the computed results. However, some discrepancies exist between the measured and simulated data, with agreement being less satisfactory than for the Case I flame, particularly in terms of the under prediction of  $\text{CO}_2$  and  $\text{H}_2\text{O}$ . Calculated results for the case with Reynolds number of 45,500 have even less satisfactory agreement with measurements (not shown here). As indicated by Prasad and Gore<sup>19</sup>,

however, these highly stretched flames lie in the distributed reaction zone, rather than the flamelet regime, where the current model is not applicable. Nevertheless, the predictions given above for the  $\text{Re} = 21,000$  flame do demonstrate the applicability of the present flamelet model to flames with relatively high stretch rates, with the flame considered lying at the border of the distributed reaction zone and flamelet regimes.

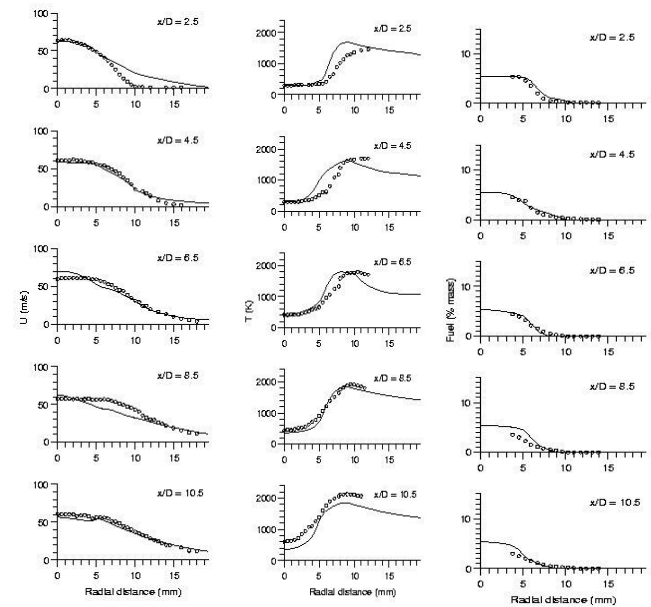


Fig. 4. Comparison of measured<sup>10</sup> and predicted mean axial velocities, temperatures and fuel concentrations at five downstream locations in the Case II flame (symbols - data, line - predictions).

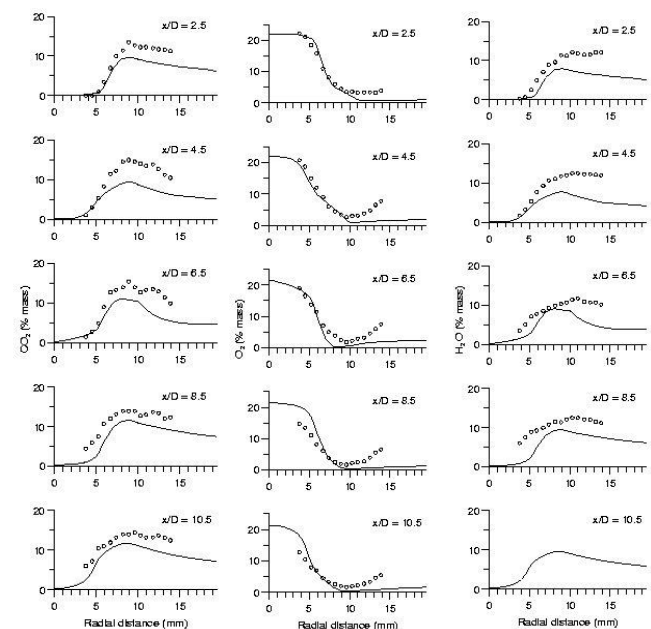


Fig. 5. Comparison of measured<sup>10</sup> and predicted  $\text{CO}_2$ ,  $\text{O}_2$  and  $\text{H}_2\text{O}$  levels at five downstream locations in the Case II flame (symbols - data, line - predictions).

Turning to the Case III flame, Figs. 6 and 7 compare predicted radial distributions of  $O_2$ ,  $CO_2$  and NO concentrations with measurements<sup>11</sup> at various axial locations. Although more limited than the data set of the Case I flame, these comparisons again demonstrate that the non-adiabatic flamelet model yields reliable predictions of major chemical species concentrations. Some deviation between predictions and observations is evident, particularly at the first measurement station where a slight lateral shift in the predictions is apparent. Centre-line  $O_2$  levels are also over predicted to some extent in the near field of the flame, and under estimated in the far field. Importantly, however, NO levels are in good agreement with data, indicating likely conformity between predicted and observed temperature values. A slight shift in the predicted NO profile at the first measurement location is again observed, although further downstream predictions largely come in line with data, and faithfully reproduce the decrease in NO levels with downstream distance.

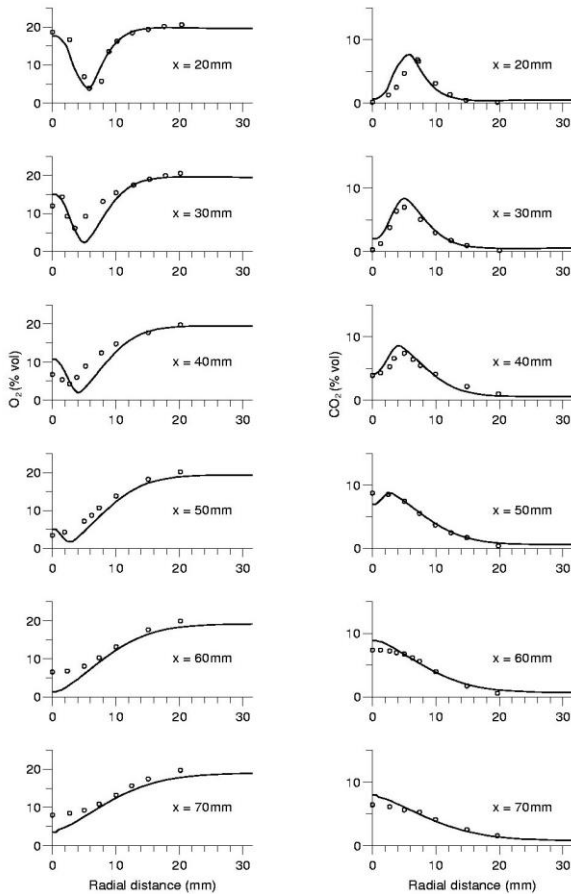


Fig. 6. Measured<sup>11</sup> and predicted  $O_2$  and  $CO_2$  levels at six downstream locations in the Case III flame (symbols - data, line - predictions).

Calculations for both flames were also performed using an adiabatic flamelet model in order to quantify the effects of radiative heat loss. The predicted results (not shown here) exhibited small differences when compared with those obtained from the non-adiabatic model. This is due to the relatively small radiative heat loss from these atmospheric pressure premixed

flames. However, at further downstream locations, where experimental data is absent, the predictions of the two models revealed larger differences, particularly for temperature and NO distributions. There is therefore a requirement for further testing of the model against idealised and practical burner flows where the influence of radiative heat loss on flame characteristics is more pronounced. This should include comparisons with data from flames enclosed within tubes where the close proximity of solid surfaces causes significant radiation heat transfer from the flame and within the enclosure itself.

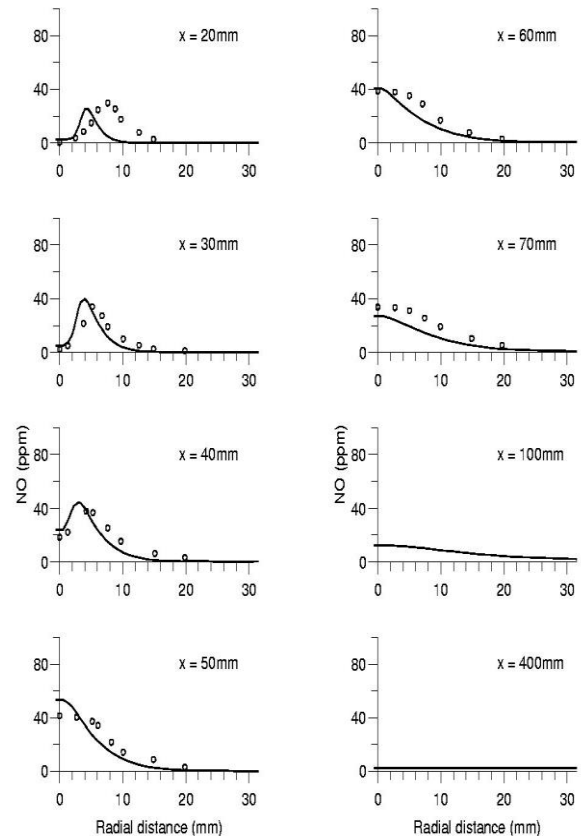


Fig. 7. Measured<sup>11</sup> and predicted NO levels in the Case III flame (symbols - data, line - predictions).

## V. CONCLUSIONS

Based on the enthalpy defect concept, the effect of radiative heat loss has been incorporated into the calculation of turbulent premixed flames using a stretched laminar flamelet modelling approach. The method has been applied in the simulation of two premixed methane-air flames, with comparisons with available data showing that the model captures the major features of these flames in terms of velocities, temperatures, major chemical species and NO concentrations. The study produces encouraging results that replicate the overall characteristics of these turbulent premixed jet flames. However, further validation is required against combustion and emission measurements in both idealised and practical burner configurations where the effects of thermal radiation on flame structure and emissions are more evident. In

addition, further extension of the model to include minor chemical species excluded from the present version is required.

#### ACKNOWLEDGMENT

The authors are indebted to the UK EPSRC for their financial support (GR/L68001/01), and to Professor D. Bradley for providing the original combustion code.

#### REFERENCES

- [1] P.A. Libby and F.A. Williams (Eds.), *Turbulent Reacting Flows*. London: Academic Press, 1994.
- [2] P.A. Libby and K.N.C. Bray, "Implication of the Laminar Flamelet Model in Premixed Turbulent Combustion", *Combust. Flame*, vol. 39, pp. 33-41, 1980.
- [3] D. Bradley, P.H. Gaskell, and X.J. Gu, "Application of a Reynolds Stress, Stretched Flamelet, Mathematical Model to Computations of Turbulent Burning Velocities and Comparison with Experiments", *Combust. Flame*, vol. 96, pp. 221-248, 1994.
- [4] D. Bradley, P.H. Gaskell, and A.K.C. Lau, "A Mixedness-Reactedness Flamelet Model for Turbulent Diffusion Flames", *Proc. Combust. Inst.*, vol. 23, pp. 685-692, 1990.
- [5] C.Y. Ma, T. Mahmud, P.H. Gaskell, and E. Hampartsoumian, "Numerical Predictions of a Turbulent Diffusion Flame in a Cylindrical Combustor Using Eddy-Dissipation and Flamelet Combustion Models", *J. Mech. Engng. Sci.*, vol. 213, pp. 697-705, 1999.
- [6] B. Marracino and D. Lentini, "Radiation Modelling in Nonpremixed Turbulent Flames", *Combust. Sci. Technol.*, vol. 128, pp. 23-48, 1997.
- [7] K.N.C. Bray, and N. Peters, "Laminar Flamelets in Turbulent Flames", In P.A. Libby and F.A. Williams (Eds.), *Turbulent Reacting Flows*, London : Academic Press, 1994.
- [8] R.J. Kee, J.F. Grcar, M.D. Smooke, and J.A. Miller, "A Fortran Program for Modelling Steady Laminar One-Dimensional Premixed Flames", *Sandia National Laboratories Report No. SAND85-8240.UC-401*, 1993.
- [9] C.L. Tien, "Thermal Radiation Properties of Gases", *Adv. Heat Transfer*, vol. 5, pp. 253-324, 1968.
- [10] Y.C. Chen, N. Peters, G.A. Schneemann, N. Wruck, U. Renz, and M.S. Mansour, "The Detailed Flame Structure of Highly Stretched Turbulent Premixed Methane-Air Flames", *Combust. Flame*, vol. 107, pp. 223-244, 1996.
- [11] H.T. Sommer, and W. Adams, "Stable Species Concentration of a Turbulent Premixed Methane-Air Flame", *Combust. Flame*, vol. 49, pp. 1-12, 1983.
- [12] B.E. Launder, and D.B. Spalding, "The Numerical Computation of Turbulent Flows", *Comp. Meth. App. Mech. Eng.*, vol. 3, pp. 269-288, 1974.
- [13] C.Y. Ma, T. Mahmud, E. Hampartsoumian, J. Richardson, and P.H. Gaskell, "Mathematical Modelling of Nitric Oxide Formation in Turbulent Diffusion Flames Doped with a Nitrogen Compound", *Combust. Sci. Tech.*, vol. 160, pp. 345-367, 2000.
- [14] Y.B. Zeldovich, P.Y. Sadonikov, and D.A. Frank-Kamenetskii, "Oxidation of Nitrogen in Combustion", *Acad. Sci. USSR, Inst. Chem. Phys., Moscow-Leningrad*, 1947.
- [15] G.G. De Soete, "Overall Reaction Rates of NO and N<sub>2</sub> Formation from Fuel Nitrogen", *Proc. Combust. Inst.*, vol. 15, pp. 1093-1102, 1975.
- [16] C.T. Bowman, R.K. Hanson, D.F. Davidson, W.C. Gardiner, V. Lissianski, G.P. Smith, D.M. Golden, M. Frenklach, and M. Goldenberg, See [http://www.me.berkeley.edu/gri\\_mech/](http://www.me.berkeley.edu/gri_mech/)
- [17] P.H. Gaskell, and A.K.C. Lau, "Curvature-Compensated Convective Transport: SMART, a New Boundedness-Preserving Transport Algorithm", *Intl. J. Numerical Methods Fluids*, vol. 8, pp. 617-641, 1988.
- [18] S.V. Patankar, *Numerical Heat Transfer and Fluid Flow*, McGraw-Hill, New York, 1980.
- [19] R.O.S. Prasad, and J.P. Gore, "An Evaluation of Flame Surface Density Models for Turbulent Premixed Jet Flames", *Combust. Flame*, vol. 116, pp. 1-14, 1999.